Nonlinear Dynamics and Applications

Proceedings of the Twenty-eight Anniversary Seminar NPCS'2021
in memory of Prof. V.I. Kuvshinov
May 18-21, 2021, Minsk, Belarus
Fractals, Chaos, Phase Transitions, Self-organization

Editors
V.A. Shaparau
A.G. Trifonov

Volume 27
2021

Nonlinear Dynamics and Applications

27

Minsk "Pravo i Ekonomika" 2021

Nonlinear Dynamics and Applications

Proceedings of the Twenty-eight Anniversary Seminar NPCS'2021

in memory of Prof. V.I. Kuvshinov

May 18-21, 2021, Minsk, Belarus

Fractals, Chaos, Phase Transitions, Self-organization

Editors

V.A. Shaparau

A.G. Trifonov

Volume 27
2021

Minsk "Pravo i Ekonomika" 2021

УДК 53(061.3)
ББК 22.3(Англ.)
Н72

Nonlinear Dynamics and Applications : Proceedings of the Twenty eight Anniversary Seminar NPCS'2021, Minsk, May 18-21, 2021 = Нелинейная динамика и приложения : труды XXVIII Международного семинара, Минск, 18-21 мая 2021 г. / редкол.: В. А. Шапоров [и др.]; под ред. В. А. Шапорова, А. Г. Трифонова; Объединенный институт энергетических и ядерных исследований – «Сосны» НАН Беларуси. – Минск : Право и экономика, 2021. – 544 с. – ISBN 978-985-552-976-8.

УДК 53(061.3)
ББК 22.3(Англ.)

ISBN 978-985-552-976-8

Научное издание

Nonlinear Dynamics and Applications : Proceedings of the Twenty eight Anniversary Seminar NPCS'2021, Minsk, May 18-21, 2021 = Нелинейная динамика и приложения : труды XXVIII Международного семинара, Минск, 18-21 мая 2021 г.

Технический редактор *В.Г. Гавриленко*

Подписано в печать 27.08.2021 Формат 60x84 1/8 Бумага офсетная
Печать цифровая Усл.печ.л. 68,03 Уч.изд.л. 68,4 Тираж 75 экз. Заказ 3974
ИООО «Право и экономика» 220072 Минск Сурганова 1, корп. 2 Тел. 8 029 684 18 66
Отпечатано на издательской системе Gestetner в ИООО «Право и экономика»
Свидетельство о государственной регистрации издателя,
изготовителя, распространителя печатных изданий, выданное
Министерством информации Республики Беларусь 17 февраля 2014 г.
в качестве издателя печатных изданий за № 1/185

ISBN 978-985-552-976-8

Contents

Preface

The 28th Anniversary International Seminar "Nonlinear Phenomena In Complex Systems" was held in memory of Prof. V.I. Kuvshinov on May 18-21, 2021, in Minsk, Belarus.

The bright memory of

Vyacheslav Ivanovich Kuvshinov

will forever remain in our hearts.

The 28th Anniversary International Seminar traditionally had subsubjects: "Fractals, Chaos, Phase transitions, Self-organization", plenary session and the following section sessions: Particles, Modelling and Safety Related Analyses of NPP, Quantum and Classical Electrodynamics, Gravity, Media, Medicine, Biological and Chemical systems, Mathematics and Fields. 14 plenary, 48 section and 7 poster reports were submitted to the 28th Seminar by the scientists. At this Anniversary Seminar, the participants gave overview reports, which became useful to young scientists. Thus, in addition to the scientific component, the seminar also played an educational role. Most of the papers were included into these Proceedings.

The 28th Anniversary Seminar 'NPCS' was supported by National Academy of Sciences of Belarus.

Nonlinear Dynamics and Applications. Vol. 27 (2021) 66 - 73

Gamma-Ray Scattering in a MWCNT Bilayer

H.V. Grushevskaya,* A.I. Timoshchenko,† and I.V. Lipnevich
Physics Department, Belarusian State University,
4 Nezalezhnasti Ave., 220030 Minsk, BELARUS

A scattering of gamma-quanta on bilayer of multiwalled carbon nanotubes (MWCNTs) has been studied. It have been shown that there are two types of graphene gamma-quanta scattered centers. We testify a topologically non-trivial Majorana-like feature for the graphene charge carriers.

PACS numbers: 72.80.Vp, 61.82.-d, 61.80.Ed, 78.67.Ch, 87.50.Gi
Keywords: graphene radiation resistivity, Majorana-like fermion charge carriers, carbon nanotube

1. Introduction

Applications of graphene-like materials in nuclear technologies are high prospective due to high mobility of the charge carriers [1, 2]. Among them, the development of radiation-resistant materials and of protective shielding nanostructured coatings is in a great demand [3]. It has been shown that graphene is stable to irradiation because the atoms of graphene do not knock out from the graphene plane. Formally, a flux density of graphene charge carriers can be infinitely high due to zero energy of electron-hole pairs producing in touching points of graphene valence and conducting bands. The touchings are called the Dirac points. Massless graphene charge carriers are high mobile even in comparison with electrons of the ordinary metals because valleys K, K' of the graphene Brillouin zone hold a nontrivial topology. The non-abelian charge transport in graphene possesses the features of statistics of pseudo-Majorana particles with nontrivial topology. The topologically nontrivial defects obey non-abelian statistics and are described by the equations of Majorana type. Therefore the mechanism of radiation resistance of graphene can be consist in interaction of gamma-quanta with super-dense fluxes of graphene charge carriers of the Majorana type. However, an interaction between gamma-quanta and the charge carriers in the graphene plane leading to a large Compton effect has not been studied yet. In this paper we investigate γ-ray affects on rolled graphene atomic layer (monolayer) of high-ordered carbon nanotube bundles.

The goal of the paper is to reveal radiation high-energy defects of a type of a pair vortex – antivortes in electron and hole densities. The fluxes of the graphene quasiparticle pairs are produced by gamma-quanta in a Coulomb field of the graphene plane.

*E-mail: grushevskaja@bsu.by
†E-mail: a_timoshchenko@mail.ru

2. Materials and methods

2.1. Materials

Carboxylated and stearic-acid-functionalized multiwalled carbon nanotubes (MWCNTs) under 2.5–5 nm in diameter have been decorated by nanocyclic complexes (Fe(II)DTP) of Ce and/or high-spin octahedral Fe with ligands being conducting oligomer of dithionylpyrrole series in the following way. As a preliminary, an alkyl hydrocarbon chain $C_{16}H_{33}$ was linked chemically to the oligomer. Chemical formula of the oligomer has the following form: 3-hexadecyl-2,5-di(thiophen-2-yl)-1H-pyrrole (H-DTP). A 5-monolayer graphene-like film of the nanocyclic organometallic complexes is fabricated by means of LB-nanotechnique. Then, inverse micelles of stearic acid with MWCNTs inside are obtained by mixing stearic acid and MWCNTs in hexane by the ultrasound treatment, and 2-monolayer MWCNT films fabricated from these micellar MWCNTs by the Langmuir–Blodgett (LB) nanotechnique are deposited on the nanocyclic-complex LB-cover. The MWCNT LB-bundles nondecorated/decorated by organometallic complexes or the LB-films of nanocyclic organometallic complexes were deposited on the interdigital structure of aluminium electrodes, on the surface of which a layer of nanoporous anodic alumina (AOA) were previously formed as a insulator coating.

2.2. Methods

2.2.1. Exposure to radiation

A low-intensive source of ionizing radiation (IRS) ^{137}Cs (CsJ), activity of radioactive decay A_0 on the date 1 April 1990 – 124.4 kBq and, accordingly, the activity at the measurement moment ($t = 30$ years) is

$$A_x = A_0 \exp(-t \ln 2/T_{1/2}) = A_0/2.$$

Here $T_{1/2}$ is half-life, $T_{1/2} = 30$ years.

The radiation of low-intensive beta-particles beam has been attenuated by a thin-film aluminium screen. The IRS has the form of a drop with a mean diameter about $d = 1.5$ mm. A sample with a diameter $D_s = 4$ mm is exposed through a collimator being of the order of 5 mm in diameter and $L = 50$ mm long. At ratio $d/L = 0.03$, IRS can be considered as a point source. MWCNTs were exposed to radiation for 1 hour.

2.2.2. Radiation spectroscopy

Analysis of secondary electrons spectra has been performed by a lab-quality radiation spectrometric facilities "Nuclear Physics" (BSU, Minsk, Belarus). The scintillation crystal thallium-activated sodium iodide, NaI(Tl) (a diameter of 25 mm, a height of 40 mm) was utilized as a detector crystal. The technical characteristics of the radiation spectrometer are the following. A photoelectric-multiplier (PEM) supply voltage U changes from 100 to 1000 V; the voltage stability does not exceed 0.05% for 5 hours of apparatus continuous work after 20 minutes warming; the admissible load current of PEM power supply is not less than 5 mA; the input resistance of the main amplifier is 15 kOm; the amplifier gain changes from 1 to 100 smoothly or stepwise; the transformable signal range is from 0 to 10 V; the signal polarity is arbitrary (it is defined programmatically in the option of amplifier gain setting); the front of signal rise is not less than 0.3 μs; the maximal signal

duration is 20 μs; a time of transformation and data translation in a computer is 30 μs accounting interlock circuit; the channels number is 1024; the differential nonlinearity is not worth than $\pm 1\%$; the integral nonlinearity (transducer characteristic error) is not more than 0.1%; the stability of photopeak position is not more than 1% for measurements of 661.7-KeV ^{137}C gamma-ray at load change by 10 times.

The number of gamma-quanta N_{event} scattered in the detector crystal has been calculated by summation of all registered pulses as

$$N_{event} = \sum_{i=Ndown+1}^{N_{up}} n_i$$

for $U = 650$ V. Here n_i is a number of pulse counts in i-th channel, the region (the number) of the low level channels is from 1 to $N_{unl} = 34$, the region of high level channels is from 1 to $N_{up} = 1000$.

3. Experimental

3.1. Radiation spectral analysis

Let us analyze MWCNT effects on incoming ^{137}Cs gamma-quanta beam. Figs. 1,2 and Table demonstrate the features of the radiation spectra under investigation. After placing of the electromagnetic-radiation absorber with MWCNT bundles decorated by the organometallic compound into the collimator, three additional lines reveals in ^{137}Cs-radiation spectrum of secondary electrons for the crystalline detector along with the backscattering peak, photopeak, and Compton line. The spectra indicate narrowing of the ^{137}Cs-radiation lines. The number of gamma-quanta $\overline{N}_{Cs}$ emitted by the ^{137}Cs radiation source is

$$\overline{N}_{Cs} = \sum_{i=Ndown+1}^{N_{up}} n_i = 5429 \qquad \text{pulses per hour.}$$

The background scattering is practically absent in high-energy channels (see Fig. 1d). The number of background events $\overline{N}_{bg}$ registered by crystal detector in the absence of the source and absorber equals

$$\overline{N}_{bg} = \sum_{i=Ndown+1}^{N_{up}} n_i = 238 \qquad \text{pulses per hour.}$$

Distributions of scattered gamma-quanta over detector channels are obtained by subtracting background from the original experimental data. The radiation spectra are represented in Figs. 1a,b. Subtracting the total radiation background from the experimental data, we find that approximately the numbers $N_{Cs} = 5191$ and $N_{Cs/CNT} = 5111$ of gamma-quanta per one hour pass through the collimator before and after the deposition of the absorber sample underneath the collimator, correspondingly. Now one can find the total decrease N_{ab} of gamma-quanta number in all channels: $N_{ab} = 80$ pulse per hour. The thickness of the MWCNT bilayer which absorbs without re-emission or reflects 80 gamma-quanta per hour, is $d_{CNT} = 5$ nm. Then the graphene monolayer of atomic thickness ($d_G = 0.1$ nm) absorbs gamma-quanta more than

$$N_G = N_{ab} d_G / d_{CNT} = 1.6 \text{ hour}^{-1}.$$

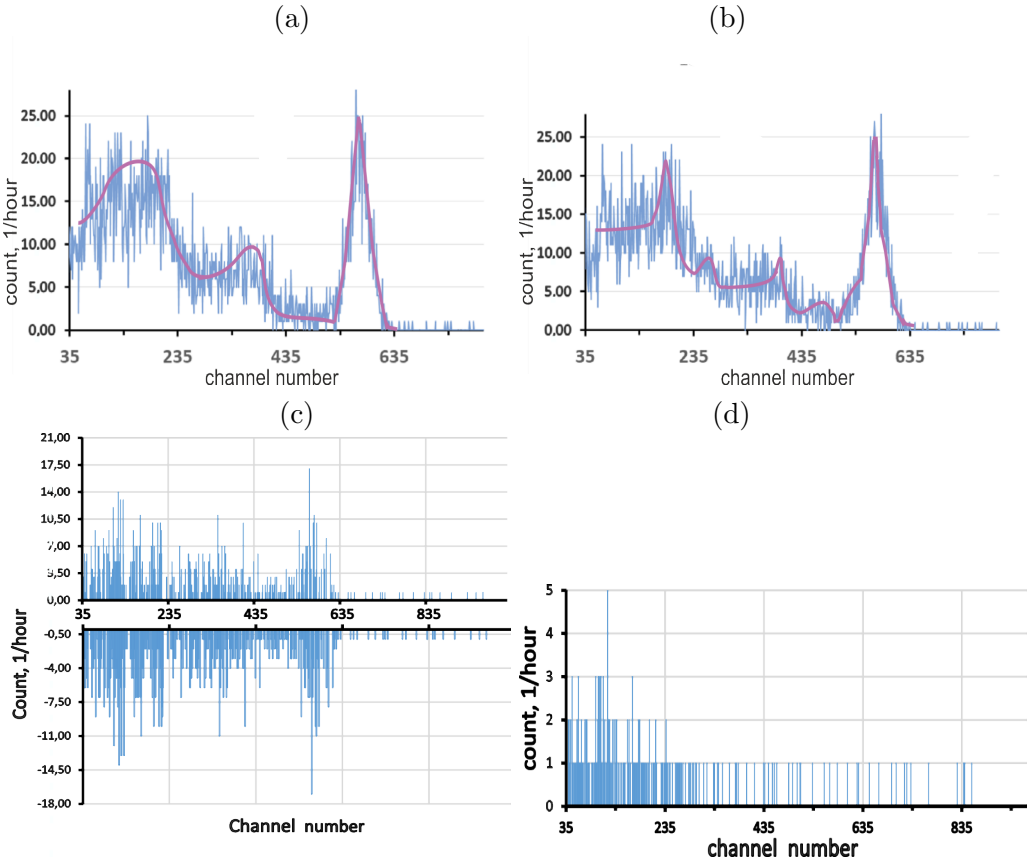

Figure 1. (color online) Channel distributions F_{Cs} (a) and $F_{Cs/CNT}$ (b) of secondary electrons produced by ^{137}Cs gamma-quanta scattering on crystal detector for beam incoming through collimator without and with MWCNT bilayers, respectively; a radiation background has been subtracted from origin distributions. (c) Difference between the distributions F_{Cs} and $F_{Cs/CNT}$. (d) The radiation background.

If we take into account a large distance between graphene monolayers, then $N_G > 2$. It signifies that the collision process proceeds predominantly in the graphene plane. So, two monolayers of MWCNTs with small number of walls absorb fully and/or reflect $N_{ab} = 80$ gamma-quanta per hour. As $N_G > 1$, the collisionless path $\lambda < d_G$, and, correspondingly, the collisions between gamma-quanta and carbon atoms happen in the graphene plane. Such ultrashort distance between collisions in the graphene plane testifies the high density of graphene charge carriers.

We observe three new bands in the spectrum of gamma-quanta scattered on the MWCNT sample and the detector crystal. Maxima of these bands are approximately in 260-th, 460-th and 535 channels (compare figs. 1a and 1b). It testifies the additional scattering and re-emission of gamma-quanta on the graphene charge carriers. The intensities of the Compton part of ^{137}Cs radiation spectrum with maximum being approximately in 360-th channel and the back-scattering peak narrow after placing of the MWCNT sample into the collimator.

Further analyzing the back scattering and Compton effect in the MWCNT bundles we reveal Majorana signs for graphene charge carriers. Let us estimate the magnitude of the scattering angle and symmetrical properties of the collision process as well as the presence of preferable directions of the scattering. To do this we subtract the number of collisions occurring in the MWCNT/detector-crystal and registered in the i-th channel from the

Table 1: Shifts of ^{137}Cs bands by the graphene absorber.

Numbers of origin and redistributed ^{137}Cs bands	Averaged origin-channel number	Averaged redistributed-channel number	Band shift
1, $\overline{1}$	40	36	−4
2, $\overline{2}$	56	63	+7
3, $\overline{3}$	65	67	+2
4, $\overline{4}$	73	82	+9
5, $\overline{5}$	85	88	+3
6, $\overline{6}$	92	93	+1
7, $\overline{7}$	94	102	+8
8, $\overline{8}$	107	112	+5
9, $\overline{9}$	119	121	+24
10, $\overline{10}$	124	142	+18
11, $\overline{11}$	158	191	+33
12, $\overline{12}$	169	165	−2
13, $\overline{13}$	196	201	+5
14, $\overline{14}$	198	311	*+113*
15, $\overline{15}$	203	233	+30
16, $\overline{16}$	218	269	+51
17, $\overline{17}$	261	338	+77
18, $\overline{18}$	283	323	+40
19, $\overline{19}$	313	361	+48
20, $\overline{20}$	333	421	*+88*
21, $\overline{21}$	351	446	*+84*
22, $\overline{22}$	367	395	+28
23, $\overline{23}$	404	559	*+154*
24, $\overline{24}$	548	581	+33
25, $\overline{25}$	563	567	+4
26, $\overline{26}$	573	585	+12
27, $\overline{27}$	597	600	+3
28, $\overline{28}$	602	6035	+1

number of collisions in the crystal without MWCNTs and registered in the same i-th channel. The results are shown in the diagram in Fig. 1c. One can see that redistribution of gamma-quanta after them collisions with the MWCNT bilayer occurs practically in all channels. To estimate parameters of the graphene scattering centers we choose the main directions along which the redistribution occurs as the directions with gamma-quanta number more than 6.

The channel groups in which gamma-quanta are accumulated originally, can be far away or enough close to the groups of channels in which gamma-quanta are detected after interaction with MWCNTs (see Table). It signifies that the scattering on MWCNTs can change the scattering angle both on small or large values. Let us to characterize the position of the pulse group by averaged values of numbers of original channels and relocated channels belonging to the same group. These averaged channel numbers for the origin and redistributed ^{137}Cs-channel number groups and also the values and directions

of their shifts with regard to each other are represented in the Table.

Now, utilizing the estimations, one can describe the types of the graphene charge carriers. According to the Table, interacting with the graphene charge carriers the gamma-quanta scattered in crystal detector into the channels of bands, labeled by numbers from 14 to 24, are redistributed in the bands with channels of higher numbers. It testifies that the gamma-rays are polarized after passing through the absorber. The beam polarization is stipulated by the pseudo-spin polarization of the graphene charge carriers in the MWCTN bundle. The origin Compton-effect bands, for example with numbers 15 and 16, turn to the bands $\overline{15}$ and $\overline{16}$ with maximum near 260th channel of the Compton-effect area so that in average the channel number changes from 215 to 260. High value of the shift (+45) testifies the presence of high-energy graphene charge carriers.

Apart this, the scattering of gamma-quanta to an enormous angle in three channel areas: near 311th channel, a region of channels "421" and "446", near 559th channel, has been observed. The absorber band with maxima near 460th channel reveals through the redistribution of bands 20 and 21 into bands $\overline{20}$ and $\overline{21}$. Huge values of the shifts (+88) and (+84) in regard with the origin bands indicate the scattering on the super-massive and super-extended charge carriers in the graphene plane. The photons originally registered in 14th and 23th bands of the back scattering and Compton effect, respectively, after the interaction with MWCNTs are detected in the vicinity of the bands $\overline{14}$ and $\overline{23}$ shifted from the origin to (+113) and (+154), respectively (see Table). The locations of the bands $\overline{14}$ and $\overline{23}$ correlate with the positions of the absorb bands which maxima are near 260th and 530th channels.

Thus, the three absorber peaks represent the graphene radiation defects. The large scattering angles and, accordingly, enormous scattering cross-section indicate super-massiveness and super-extent of the defects. Apart this, to gamma-quanta interact efficiently with the defects the latter should not escape from the graphene plane. Topologically nontrivial pseudoMajorana fermions and antifermions hold such features, and the conservation law prohibits them to leave the graphene plane.

PseudoDirac electrons and holes represent themselves the superpositions of the pseudoMajorana quasiparticles. These high-energy electron-hole configurations are responsible for the scattering of gamma-quanta in to lower angles than previously considered but yet large enough angles in the graphene absorber. Besides a moderate number of the Majorana channels, all other channels are the graphene–pseudoDirac–electron channels. The gamma-quanta redistribution is related to the pseudoDirac channels at the channel-number change smaller than 80. (see Table). Meanwhile, the increment of the scattering angles due to collisions between these low-energy graphene charge carriers and the gamma-quanta can take the negative values. Because of that one can assume that the part of high-energy graphene charge carriers exists for a long enough time to be depolarized interacting each other and expending the energy in re-emission of the gamma-quanta. Because the long-lived high-energy graphene scattering centers constitute the majority of the high-energy population, they are the electrons of the secondary graphene electron-hole pairs which are avalanche-likely produced at fusion of short-lived high-energy graphene pseudoMajorana defect and antidefect. Since there exists an avalanche of these secondary graphene electrons the graphene material is an high-performance radiation shield.

So, two types of the high-energy scattering centers are observed in the graphene. Since the Compton scattering on them occurs predominantly with the change of channel number in direction of positive values, the graphene charge carriers are polarized.

4. Results and discussion

In an alternating electric field of gamma rays the vorticities of the charge carriers density near the graphene valleys are "featherings" of the vortexes whose cores reside in the Dirac point. The statistics of such topologically nontrivial defects is nonabelian one and their quasi-particle excitations are pseudo-Majorana fermions and antifermions. At the Compton scattering of gamma-quanta in MWCNT graphene planes, the production of the Majorana and anti-Majorana quasiparticles pairs leads to a gamma-quanta-energy decrease equal to the pair energy and, accordingly, to the appearance of three additional detector lines with energies less than the photoeffect energy that has been observed experimentally. The produced pairs and antipairs of the pseudo-Majorana particles can annihilate between each other likely to electrons and holes. The pseudoMajorana graphene charge carriers are massless ones in the Dirac points K, K' of graphene Brillouin zone. But out of the valleys K, K' in the conduction band and valence band one fermion (antifermion) of the valley K (K') in the pseudo-Majorana pair (antipair) remains massless while the second one acquires a mass [4].

In virtue of the conservation laws of the spirality and of the topological charge, the massless pseudoMajorana charge carriers move in a collisionless way and live long time τ until they produce pairs (antipairs) with zero topology charge. As τ is much longer than the registration time, the energy released in the detector becomes less on the energy of massless pseudoMajorana pair: $E_{p_{Majorana}} = E_\gamma - 2E_{p_{lM}}$. Here E_γ is the energy of ^{137}Cs gamma-quantum, $E_{p_{lM}}$ is an energy of the light pseudoMajorana charge carriers. This peak is denoted by "LMP" in Fig. 2. Oppositely to the massless fermion, the massive one can be stopped that results into the violation of the spirality (chirality) conservation law. Therefore, the light massless Majorana fermion (antifermion) much more faster finds and annihilates with the heavy resting pseudoMajorana antifermion (fermion) with topological charge of the opposite sign. Meanwhile the energy E_{LM} is given up to the detector through producing gamma-quanta. The magnitude of E_{LM} is a bit less than E_γ because the fast light pseudoMajorana fermion (antifermion) finds the fermion (antifermion) with opposite topological charge for a short time which is not enough to scatter the heavy pseudoMajorana fermion on the graphene electron density. The annihilation peak of the heavy and light pseudoMajorana fermions is denoted by "LM" in Fig. 2.

The heavy massive Majorana fermion (antifermion) and antifermion (fermion) also annihilate each other and gives up the energy E_{HM} to the detector. However, E_{HM} is less than E_{LM} because the nonchiral Majorana fermions take much more time to find ones with topological charges of opposite sign and, accordingly, they loss much more energy in the scattering processes on the graphene electron density. The annihilation peak of two heavy pseudoMajorana fermion and antifermion is marked by "HM" in Fig. 2.

The calculation of the linear attenuation coefficient for the gamma-quanta flux .

For the nuclear applications the estimation of the MWCNT ability to radiation shielding is important. Let us to calculate the linear attenuation coefficient μ of the gamma-quanta flux from J_0 to J that is defined by the following formula:

$$J = J_0 \exp(-\mu \Delta x),$$

where Δx is the absorber thickness. Since the two-monolayer MWCNT film of the thickness Δx 5 nm is very thin, the gamma-quanta-flux diminishing on 80 pulses per hour occurs approximately with the coefficient

$$\mu = (J_0 - J)/(J_0 \Delta x) = 80/5191/(5 \cdot 10^{-9}) = 3.08 \cdot 10^6 \text{ m}^{-1}$$

and, correspondingly, the shielding MWCNT-layer of the thickness $\Delta x_{1/2} = 0.23$ μm diminishes the flux with factor two.In comparison, the layer of the half attenuation and

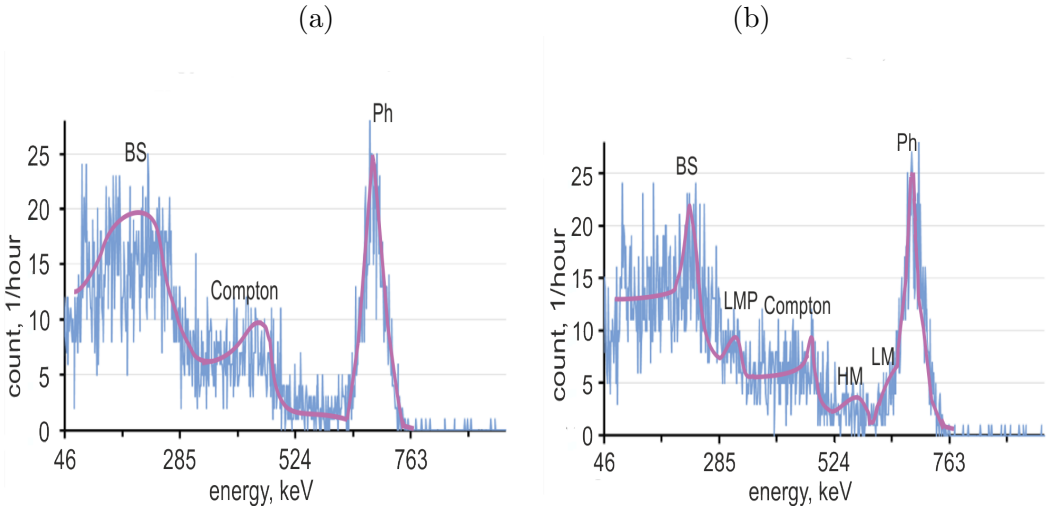

Figure 2. (color online) Energy distributions F_{Cs} (a) and $F_{Cs/CNT}$ (b) of secondary electrons produced by ^{137}Cs gamma-quanta scattering on crystal detector for beam incoming through collimator without and with the absorber, respectively. The backscattering peak, photopeak, and Compton line are called as "BS", "Ph", and "Compton"; the absorber lines are called as "LMP", "HM", and "LM".

the attenuation coefficient for the lead are equal to 1 cm= 10^4 μm and 1.18 10^2 m^{-1}, respectively.

5. Conclusion

So, scattering in MWCNTs the 661.7 keV gamma-quanta create pairs of topologically nontrivial radiation-induced defects and antidefects. These high-energy pairs of the graphene scattering centers and anticenters are pseudoMajorana fermions and antifermions. Annihilating and scattering on the carbon electron density the pseudoMajorana quasiparticles create electron-hole configurations of graphene charge density in an avalanche-like way.

References

[1] M. Ćosić, S. Petrovi, N. Nešković. Quantum rainbows in positron transmission through Carbon Nanotubes. Atoms. Vol. 7, 16 (2019).

[2] H.V. Grushevskaya, G.G. Krylov, S.P. Kruchinin, B. Vlahovic, S. Bellucci. Electronic properties and quasi-zero-energy states of graphene quantum dots. Phys.Rev. B. **103**, 235102 (2021).

[3] C.-H. Liu *et al.* Graphene photodetectors with ultra-broadband and high responsivity at room temperature. Nat Nanotechnol. **9**(4), 273 (2014).

[4] H. Grushevskaya, G. Krylov. Vortex Dynamics of Charge Carriers in the Quasi-Relativistic Graphene Model: High-Energy $\vec{k} \cdot \vec{p}$ Approximation. Symmetry. **12**, 261 (2020).

Author index